

## Size, Shape, and Low Energy Electronic Structure of Carbon Nanotubes

C. L. Kane and E. J. Mele

*Department of Physics, Laboratory for Research on the Structure of Matter, University of Pennsylvania, Philadelphia, Pennsylvania 19104*

(Received 27 August 1996)

A theory of the long-wavelength low-energy electronic structure of graphite-derived nanotubes is presented. The propagating  $\pi$  electrons are described by wrapping a massless two dimensional Dirac Hamiltonian onto a curved surface. The effects of the tubule size, shape, and symmetry are included through an effective vector potential which we derive for this model. The rich gap structure for all straight single wall cylindrical tubes is obtained analytically in this theory, and the effects of inhomogeneous shape deformations on nominally metallic armchair tubes are analyzed. [S0031-9007(97)02693-8]

PACS numbers: 61.46.+w, 71.20.Tx, 73.20.Dx, 85.40.Ux

Since the discovery of a new family of carbon based structures formed by folding graphite sheets into compact tube-shaped objects, there has been interest in the electronic properties which can be realized with these structures [1]. It is now understood that these tubes exhibit insulating, semimetallic, or metallic behavior depending on the helicity of the mapping of the graphite sheet onto the surface of the tube [2–5]. Discrete microscopic defects, in the form of disclination pairs, provide an interface between neighboring straight tubule segments of *different* helicities with different electronic gaps, providing a novel class of elemental heterojunctions [6].

In this Letter we investigate the effects of shape fluctuations on the electronic properties of the carbon nanotubes. We present a new formulation of this problem which allows us to study the effects of geometry on the quantum dynamics for a  $\pi$  electron propagating within the surface of the wrapped graphite sheet. We show that the very rich gap structure already well established for straight single wall cylindrical tubules can be derived directly from this geometrical theory [2–5]. We then extend the model to consider the effects of *inhomogeneous* deformations in the form of local twists and bends of the tubule on the low-energy electronic structure. These are important low-energy structural degrees of freedom of the tubules, and indeed one finds that these deformations are easily quenched into any three dimensional network composed of tubules. We show that these shape fluctuations also have a very strong effect on the low-energy electronic and transport properties.

An isolated two dimensional sheet of graphite is a semimetal, with the Fermi energy residing at a critical point in the two dimensional  $\pi$  electron spectrum. The Fermi surface is collapsed to a point for this system; there are two distinct Fermi points at  $K$  ( $K'$ ) points of the zone ( $\pm 4\pi/3a, 0$ ), where  $a$  is the length of the primitive translation vector ( $a = \sqrt{3}d$  where  $d$  is the nearest neighbor bond length of the graphite lattice). Expanding the  $\pi$  electron Hamiltonian around either of these points one finds that the low-energy electronic

states are described by a massless two dimensional Dirac Hamiltonian,  $H_{\text{eff}} = v\vec{\sigma} \cdot \vec{p}$ , where  $p$  denotes a two dimensional momentum in the graphite plane, and the  $\sigma$ 's are the  $2 \times 2$  Pauli matrices [7]. Here the two spin polarizations of the particle refer to the two independent basis states (labeling the  $a$  and  $b$  sublattices) in the graphite primitive cell. Thus, in addition to its physical spin and momentum, the  $\pi$  electron carries an internal pseudospin index, labeling the sublattice state, and an isospin index, labeling the two independent Dirac spectra derived from the  $K$  and  $K'$  points of the zone. The Fermi energy for this system is at  $E = 0$ .

To study the electronic behavior of the tubule one maps  $H_{\text{eff}}$  onto a curved surface. The mapping of the graphite sheet onto the cylindrical surface can be specified by a single superlattice translation vector  $T_h$  which defines an elementary orbit around the waist of the cylinder. In the absence of disclinations the superlattice vector  $T_h$  is an element of the original graphite triangular Bravais lattice. This wrapping is conventionally indexed by two

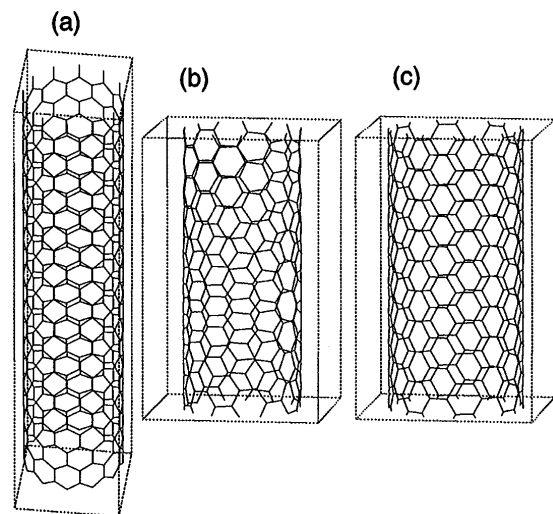


FIG. 1. Lattice structures for (a) the ideal zigzag [12,0] tube, (b) the ideal chiral [8,6] tube, and (c) the ideal armchair [8,8] tube.

integers  $[m, n]$  such that  $T_h = mT_1 + nT_2$  with  $T_1 = a(1, 0)$  and  $T_2 = a(1/2, \sqrt{3}/2)$  [2–5]. In Fig. 1 we show the structures of three cylindrical single wall nanotubes for selected values of  $m$  and  $n$ . The  $\pi$  electron eigenstates  $\Psi(r)$  satisfy periodic boundary conditions on the cylinder, i.e.,  $\Psi(r + T_h) = \Psi(r)$ . Interestingly this does *not* imply periodic boundary conditions for the eigenfunctions of  $H_{\text{eff}}$ . Instead,  $H_{\text{eff}}$  is obtained from a factorization of the single particle state  $\Psi = \psi(r) \cdot [U_a(r), U_b(r)]$  where  $(U_a, U_b)$  are the two sublattice components of the eigenstates of the  $\pi$  electron Hamiltonian at the critical  $K$  point of the zone, and  $\psi(r)$  is a (slowly varying) eigenstate of  $H_{\text{eff}}$ . In particular, the functions  $U_a$  and  $U_b$  are Bloch functions with crystal momentum  $K = (4\pi/3a, 0)$  which do not retain the periodicity of the original Bravais lattice, but are invariant only under the translations of a  $\sqrt{3} \times \sqrt{3}$  superlattice. Since  $\Psi(r)$  is invariant under Bravais lattice vector  $T_h$ , one finds that the function  $\psi$  is conjugate to  $U$ , and accumulates a phase  $e^{-iK \cdot T_h}$  under translations  $T_h$ .

This phase shifted boundary condition is an awkward computational as well as conceptual constraint on the low-energy theory. However, we observe that this constraint can always be enforced by imposing strictly periodic boundary conditions on the wave function  $\psi$  in the presence of an effective vector potential  $a_w$  which satisfies  $2\pi \int a_w \cdot dl = -K \cdot T_h$  where the line integral is taken on a closed orbit around the waist of the cylinder. This vector potential can be associated with an elementary flux of strength  $\Phi = -K \cdot T_h/2\pi$  which links the cylinder.

The azimuthal quantum states which satisfy periodic boundary conditions on the surface of the cylinder are the cylindrical harmonics  $e^{im\phi}$  with integer  $m$ . We adopt a coordinate system in which the  $\xi$  direction denotes the (counterclockwise) tangential direction on the tube's surface, and the  $\zeta$  direction is aligned along the tube. Then for the  $m$ th channel propagating along the tubule

$$H_{\text{eff}} = \frac{2\pi v}{T_h} \sigma_1(m + \Phi) - iv\sigma_2\partial_\zeta, \quad (1)$$

with spectrum  $E = \pm v\sqrt{q_\zeta^2 + (2\pi/T_h)^2(m + \Phi)^2}$ . Thus, for any wrapping where  $\Phi$  is an integer, the accumulated phase due to the vector potential can be absorbed into the definition of the azimuthal quantum number  $m$ . In particular, there exists an azimuthal state  $m = -\Phi$  for which the “mass” term vanishes, and the electronic spectrum is gapless. This occurs for the wrapped tubules in which  $T_h$  is an element of a regular  $\sqrt{3} \times \sqrt{3}$  superlattice of the original graphite Bravais lattice. For the remaining two-thirds of the wrapped structures, the minimum value of  $|m + \Phi| = 1/3$ , so that these structures retain a nonvanishing gap  $\Delta E = 4\pi v/3T_h$ . In a nearest neighbor tight binding model, with nearest neighbor hopping amplitude  $t$ , one has  $v = 3td/2$  so that these primary gaps depend inversely on the tube radius  $R$ ,  $\Delta E = td/R$  as has already been deduced from numerical work by several groups and derived analytically from a tight

binding model [5]. It is noteworthy that the symmetry of the Dirac spectrum requires that for the metallic tubules for each isospin there is only a single azimuthal branch of the electronic spectrum which crosses the Fermi energy, *independent* of the radius of the tubule, and that transport in a single tube is therefore always governed by a single transverse channel.

In addition to the wrapping constraint described above, the local *shape* of the tubule plays an essential role in determining the low-energy electronic properties. Specifically, curvature and shear in a graphite sheet introduce variations in the local electronic hopping amplitudes. Consider fluctuations in the hopping amplitudes  $\delta t_a$  along three nearest neighbor bonds  $\vec{\tau}_a$  at a given site on sublattice  $a$ . The average value of  $\delta t_a$  simply renormalizes the velocity of the Dirac particle. However, the variation from bond to bond introduces a new symmetry breaking term in the form  $\delta H_{\text{eff}} = (v/2)(a_c^+ \sigma^- + a_c^- \sigma^+)$ , where

$$a_c^\pm = \frac{1}{v} \sum_{a=1}^3 \delta t_a e^{\pm i\vec{k} \cdot \vec{\tau}_a} \quad (2)$$

and  $\sigma^\pm = \sigma_1 \pm i\sigma_2$ . Defining the vector

$$\vec{h} = \sum_{a=1}^3 \hat{\tau}_a \delta t_a/t, \quad (3)$$

it is straightforward to show  $a_c^\pm = i(2/3d)(h_x \pm ih_y)$ . This term may be written as an effective curvature derived vector potential [8]  $\vec{a}_c = \hat{z} \times \vec{h}$ , where  $\hat{z}$  is the local unit normal vector. We then have

$$H_{\text{eff}} = v\vec{\sigma} \cdot (\vec{p} + \vec{a}_w + \vec{a}_c). \quad (4)$$

A similar expression may be derived for the  $K'$  point. Equation (4) demonstrates that the effect of fluctuations in the bond hopping amplitudes are to displace the singular point of the Dirac operator in  $k$  space, but not to remove it. As an electron propagates on the surface of a tube it accumulates a phase from both the winding condition (through  $a_w$ ) and from the local fluctuations of the hopping amplitudes (through  $a_c$ ) which it encounters along its path.

The bond hopping fluctuations can now be analyzed by studying the bond length variations and the misorientation of  $\pi$  electron orbitals on neighboring sites of the tubule. The detailed calculations leading to the results given below are straightforward but lengthy [9], and will not be presented here. Instead we focus on the key results. One finds that the dependence of the hopping amplitudes on bond length for a hop along bond  $\vec{\tau}_a$  can be expressed in terms of the metric tensor  $g_{ij}$  for the curved surface so that

$$\delta t_a/t = (\beta/2d^2)\tau_a^i \tau_a^j (g_{ij} - \delta_{ij}), \quad (5)$$

where  $\beta = \partial \ln t / \partial \ln d$  gives the linear dependence of the bond hopping operator on bond length. We consider the  $\pi$  orbitals to be oriented along the local normal of the tubule surface. On a curved surface, the local normals

on two neighboring sites are no longer perfectly aligned, and this misorientation also modulates the hopping amplitudes. We find that this effect can be calculated using both the metric tensor  $g_{ij}$  and the curvature tensor  $K_{ij}$  [10]. The result is

$$\delta t_a/t = -(1/8)\tau_a^i \tau_a^j K_{jk} K_{il} g^{kl} + \dots \quad (6)$$

There is an additional contribution which arises from rehybridization of the  $\pi$  electron states on the curved manifold, and it can be derived by studying the effects of shape fluctuations on the invariant  $(\hat{n} \cdot \vec{\tau}_a)(\hat{n}' \cdot \vec{\tau}_a)$  [9]. The essential ingredients for the long-wavelength physics are already contained in the former two contributions, and we now consider them in more detail.

For a tubule in the form of a right circular cylinder we need to specify the metric tensor, curvature tensor, and the tipping angle  $\theta$  which orients a bond of the honeycomb network with respect to the “ $\zeta$  axis” along the length of the tube. For the right circular cylinder we have  $g_{ij} = \delta_{ij}$  and the only nonzero component of the curvature tensor is  $K_{\xi\xi} = 1/R$ . Thus the pure metric contribution to  $\vec{a}_c$  vanishes, and we only have the orientational contribution. The explicit form may be found using (3) and (6) along with the fact that for any three vectors  $\vec{A}$ ,  $\vec{B}$ ,  $\vec{C}$ ,  $\sum_a (\hat{\tau}_a \cdot \vec{A})(\hat{\tau}_a \cdot \vec{B})(\hat{\tau}_a \cdot \vec{C}) = (3/4)\text{Re}[A^+ B^+ C^+]$ . Expressing  $\vec{a}_c$  in the new coordinate system, we find  $a_c^+ = a_{c\xi} + ia_{c\zeta} = -e^{3i\theta} d/16R^2$ . Note that this contribution is proportional to the square of the tubule curvature, and is unchanged under rotations of the tipping angle by  $2\pi/3$  as one expects from the symmetry of the honeycomb lattice. For the “zigzag” tubes [as shown in Fig. 1(a)] we have a bond exactly aligned with the long axis of the cylinder, so that  $\theta = 0$  and  $a_c^+$  is purely real. This means that  $\vec{a}_c$  is directed along the circumferential direction of the tube. Here the line integral  $\int a_c \cdot dl$  around the waist of the tube is nonvanishing (and in general nonintegral), so that the curvature makes a nonzero contribution to the effective mass of the Dirac particle in Eq. (4). For the armchair tubes [as shown in Fig. 1(c)]  $\theta = \pi/2$  so that the vector potential is purely imaginary, indicating that it is directed exactly *along* the tube direction. For this geometry its only effect is to rigidly shift the electronic spectrum along the  $q_\zeta$  direction in momentum space. This shift has no physical consequence and can be completely eliminated from this geometry by a simple gauge transformation. Since  $\Phi$  is an integer for all armchair tubes, and the curvature corrections can be removed from the Hamiltonian by a gauge transformation, the mass term vanishes and all the straight armchair tubules remain metallic.

For a given cylindrical tubule the total band gap is  $|2\nu(a_w + \text{Re}[a_c^+])|$ , and in Fig. 2 we display a plot of the total gaps predicted for all tubules with radii less than 15 Å. The plot identifies three distinct families of tubules: (a) tubes with primary winding induced gaps scaling as  $1/R$  with curvature-derived fluctuations scaling as  $1/R^2$  [11], (b) tubes with vanishing primary gaps, and a

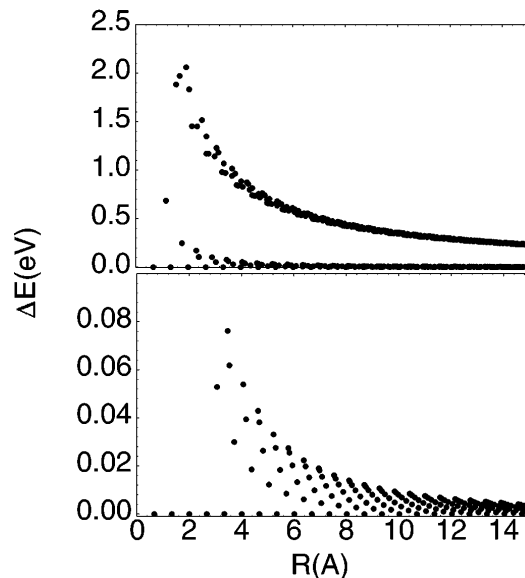


FIG. 2. Gaps calculated for all right circular tubes with radii less than 15 Å. The tubes fall into three families: those with primary gaps which scale as  $1/R$  (top panel, top curve), those with zero primary gap but nonzero curvature induced gaps which scale as  $1/R^2$  (lower curve top panel, and shown in the expanded scale in the lower panel), and armchair tubes with zero primary gap and zero curvature induced gap.

nonvanishing curvature induced gap (these are shown on an expanded scale in the lower panel), and (c) zero gap (armchair tubules) for which both the primary gaps and curvature induced gaps vanish by symmetry. The data predicted within this model provide a strikingly complete description of numerical data for these gaps obtained from a complete tight binding analysis of these tubes employing four basis orbitals per carbon site for each of these structures [12]. We remark that the scales of these gaps for tubes of radius  $\approx 10$  Å are by no means negligible and can have important consequences for the low temperature transport properties [13].

This model can now be extended to far more complex structures which contain fluctuations in the tubule shape. Physically, just as the uniform vector potential describes a homogeneous mapping of the graphite plane onto the tubule surface, a perturbation to the tubule shape produces a perturbation in the vector potential which then can scatter a quantum particle. Here we will focus only the armchair tubes, since these are the only structures which are metallic in the absence of shape fluctuations. We consider the effects of long-wavelength twists and bends of the tubule, as shown in Fig. 3 since these are the low-energy degrees of freedom for the system.

We find that even a modest twist can serve as a strong scatterer for a propagating  $\pi$  electron. The dominant effects are introduced through the metric tensor contributions in Eq. (5). For a tube subject to a twist  $\gamma = \partial_\zeta \phi$  we find  $a_c^+ = ie^{3i\theta} \beta(R/2d)\gamma$ . For the armchair tube,  $\vec{a}_c$  is directed along the circumferential direction and provides a gap in the Dirac spectrum of  $(3\beta\gamma R/2)t$ . Physically this

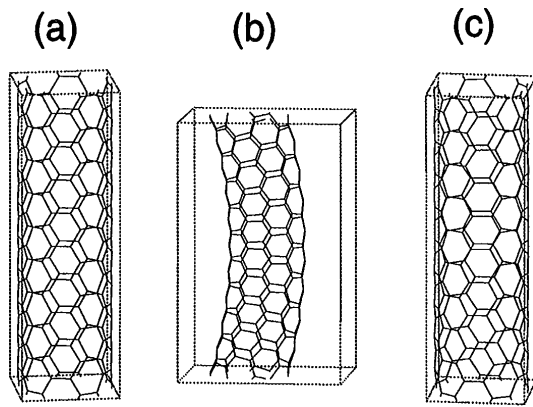


FIG. 3. Deformations of an armchair [5,5] tube. The left panel gives the ideal tube structure. The middle and right panels show the effects of uniform bend and twist on the structure.

effect is due to an asymmetric compression and dilation of the “axial” bonds on the surface of the twisted tubule. Here we find that a twist which rotates the wrapped graphite structure through an angle of  $\pi$  over a distance of  $1 \mu\text{m}$  introduces a gap of 20 meV at the Fermi surface. The contributions from the curvature induced misorientation of the  $\pi$  orbitals in Eq. (6) are considerably smaller by a factor  $d^2/12\beta R^2$ .

Interestingly, we find that the coupling to bend is much weaker. A deformation with a constant bend but no twist does not backscatter a particle. The underlying reason for this is that an armchair tube with uniform bend has a local mirror plane which preserves the symmetry between the “axial” bonds. This ensures that the effective vector potential points along the tube, so it is ineffective for backscattering a propagating particle. In principle, a propagating  $\pi$  electron can scatter from spatial variation of the bend. However, the first order coupling to the derivative of the curvature  $\partial_\xi K_{\xi\xi}$  [14] vanishes due to the azimuthal symmetry of the electronic states at the Fermi energy. From the higher order corrections we estimate a bend induced gap of order  $\epsilon R^3 d/\Lambda^4$ , where  $\Lambda$  is the persistence length of the tube, so the correction is negligible for the situation of experimental interest.

In a real single wall tubule, one expects that the twist can be inhomogeneously distributed along the tubule length. For a twisted section of tubule connecting two untwisted armchair tubes, one can regard the connecting segment as a weak link between conducting segments. At sufficiently low temperature, backscattering from these defects can ultimately lead to localization of a quantum particle. However, before this idea can be meaningfully applied to these systems, the model will have to be generalized to describe the competing effect of interwall quantum coherence in three dimensional samples built out of single wall tubes. Nevertheless we remark that recent measurements on ropes composed of armchair tubes, and on mats composed of an ensemble of connected ropes, show a resistivity which crosses over from a low temperature regime

with resistivity decreasing with increasing temperature to a high temperature regime in which the resistivity is increasing roughly linearly with temperature [15]. This crossover occurs in the range 10–200 K (depending on sample quality and morphology), and since these temperatures are in an energy range which can be easily accounted for by the shape fluctuations discussed above, it is tempting to associate this crossover with the onset of strong backscattering from quenched disorder in the tubule twist. It would be quite interesting to quantify this idea by measuring the degree of twist which is actually quenched into three dimensional samples composed of carbon nanotubes. Finally, we note that the twist can be thermally excited and provides an important temperature dependent scattering rate for  $\pi$  electrons propagating along the tubule.

It is a pleasure to thank J.E. Fischer and R. Kamien for helpful discussions. This work was supported by DOE under Grant No. DE-FG02-84ER45118, and by the NSF under Grants No. DMR 93 13047 and No. DMR 95 05425.

- [1] For a recent review, see T. Ebbeson, *Phys. Today* **49**, No. 6, 26 (1996).
- [2] J. W. Mintmire, B. I. Dunlap, and C. T. White, *Phys. Rev. Lett.* **68**, 631 (1992).
- [3] R. Saito, M. Fujita, G. Dresselhaus, and M. S. Dresselhaus, *Appl. Phys. Lett.* **60**, 2204 (1992).
- [4] N. Hamada, S. Sawada, and A. Oshiyama, *Phys. Rev. Lett.* **68**, 1579 (1992).
- [5] J. W. Mintmire, D. H. Robertson, and C. T. White, *J. Chem. Phys. Sol.* **54**, 1835 (1993).
- [6] L. Chico, V. H. Crespi, L. X. Benedict, S. G. Louie, and M. L. Cohen, *Phys. Rev. Lett.* **76**, 971 (1996).
- [7] D. P. DiVincenzo and E. J. Mele, *Phys. Rev. B* **29**, 1685 (1984).
- [8]  $\tilde{a}_c$  is not related to the spin connection for the curved surface, whose curl is the Gaussian curvature.
- [9] C. L. Kane and E. J. Mele (unpublished).
- [10] F. David, in *Statistical Mechanics of Membranes and Surfaces*, edited by D. Nelson, T. Piran, and S. Weinberg (World Scientific, Singapore, 1989), Vol. 5.
- [11] The  $1/R^2$  scaling of the curvature derived gaps for these structures has been discussed by C. T. White, D. H. Robertson, and J. W. Mintmire, in *Clusters and Nanostructured Materials*, edited by P. Jena and S. Behera (Nova, New York, 1996), p. 231.
- [12] C. T. White, J. W. Mintmire, R. C. Mowery, D. W. Brenner, D. H. Robertson, J. A. Harrison, and B. I. Dunlap, in *Buckminsterfullerenes*, edited by W. E. Billups and M. Ciufolini (VCH Publishers Inc., Weinheim and New York, 1993), Sec. 6.5, pp. 159f.
- [13] In addition for tubes of very small radius, rehybridization effects not present in the tight binding theory can intervene. See X. Blase, L. X. Benedict, E. L. Shirley, and S. G. Louie, *Phys. Rev. Lett.* **72**, 1878 (1994).
- [14] For a tube of radius  $R$  bent with a local radius of curvature  $R'$ ,  $K_{\xi\xi} = (1/R') \sin \xi/R$ .
- [15] J. E. Fischer, H. Dai, R. Lee, M. Nhajani, A. Thess, D. T. Colbert, and R. E. Smalley, *Phys. Rev. B* **55**, 4921 (1997).